Plasmonics (2015) 10:1173–1183
DOI 10.1007/s11468-015-9913-6

# Scattering of an Obliquely Incident Surface Plasmon Polariton from Sub-Micron Metal Grooves and Ridges

**J. Polanco · R. M. Fitzgerald · A. A. Maradudin**

Received: 25 November 2014 / Accepted: 16 February 2015 / Published online: 12 March 2015


**Abstract** The reduced Rayleigh equation for the scattering of a surface plasmon polariton incident non-normally on a one-dimensional ridge or groove on an otherwise planar metal surface is solved by a purely numerical approach. The solution is used to calculate the transmission, reflection, and out-of-plane scattering coefficients of the surface plasmon polariton. The angular dependence of the out-of-plane scattering is found to have a conical nature.

**Keywords** Surface plasmon · Polariton

## Introduction

In the great majority of the theoretical studies of the scattering of a surface plasmon polariton by linear surface topographical defects, ridges, and grooves, it has been assumed that the surface electromagnetic wave is incident normally on the defect [1–13]. The single exception to this general practice is the work of Nikitin and Martín-Moreno [14] who studied the scattering of a surface plasmon polariton incident obliquely on a one-dimensional surface relief defect with the use of both an approximate impedance boundary condition and a Rayleigh expansion. This scattering geometry is an important one to study because the determination of surface plasmon polariton reflection coefficients are easier to obtain experimentally in oblique incidence. In addition, the solution of the oblique incidence case constitutes the more general case.

In this paper, we present an approach to the determination of the reflection, transmission, and out-of-plane scattering coefficients of a surface plasmon polariton incident obliquely on a one-dimensional nanoscale topographical surface defect on an otherwise planar vacuum-metal interface. It is based on a purely numerical solution of the reduced Rayleigh equation for this scattering problem, and is exact when the surface profile function defining the defect satisfies the condition [15–23] for the validity of the Rayleigh hypothesis [24]. This has been discussed in our earlier work [13].

In addition to providing exact results for the reflection, transmission, and out-of-plane scattering coefficients, we also show that the out-of-plane scattered field is in fact conically scattered, a feature that has not been noted in earlier studies of this problem.

Although the incident surface plasmon polariton is *p*-polarized, the fact that it is incident obliquely on the one-dimensional surface defect means that the scattered volume electromagnetic fields have both *p*- and *s*-polarized components. Consequently, we have to work with the reduced Rayleigh equation for a two-dimensional rough surface [25].

In the form used in this paper, the reduced Rayleigh equation is applicable only to lossless metals. This is not a serious restriction because the surface plasmon polariton propagation length is in general significantly longer than the width of a nanoscale surface defect, as was discussed in [13]. It is a restriction that can be lifted at the expense of having to solve a more complicated, one-dimensional 2 x 2 matrix integral equation for the scattering amplitudes [8].

J. Polanco
Department of Mathematics, University of Texas,
El Paso, TX 79968, USA

R. M. Fitzgerald (✉)
Department of Physics, University of Texas,
El Paso, TX 79968, USA
e-mail: rfitzgerald@utep.edu

A. A. Maradudin
Department of Physics and Astronomy, University of California,
Irvine CA 92697, USA

## The Scattered Field

The system we study consists of vacuum in the region $x_3 > \zeta(x_1)$, and a metal, characterized by an isotropic, frequency-dependent, real dielectric function $\epsilon(\omega)$, in the region $x_3 < \zeta(x_1)$ (Fig. 1). We work in the frequency region where $\epsilon(\omega) < 0$, which is the frequency region in which a surface plasmon polariton exists.

The surface profile function $\zeta(x_1)$ is assumed to be a single-valued function of $x_1$ that is differentiable, and is sensibly nonzero over only a finite portion of the $x_1$ axis about its origin.

A surface plasmon polariton of frequency $\omega$ is obliquely incident on the surface defect. The electric field in the region $x_3 > \zeta(x_1)_{\max}$ is the sum of an incident and a scattered field:

$$\begin{aligned} \boldsymbol{E}(\mathbf{x}|\omega) &= -\frac{c}{\omega}[-i\beta_0(k_\parallel)\hat{\mathbf{k}}_\parallel + k_\parallel \hat{\mathbf{x}}_3]\exp[i\boldsymbol{k}_\parallel \cdot \boldsymbol{x}_\parallel - \beta_0(k_\parallel)x_3] \\ &\quad + \int \frac{d^2q_\parallel}{(2\pi)^2}\left\{\frac{c}{\omega}[i\beta_0(q_\parallel)\hat{\mathbf{q}}_\parallel - q_\parallel \hat{\mathbf{x}}_3]A_p(\boldsymbol{q}_\parallel) + (\hat{\mathbf{x}}_3 \times \hat{\mathbf{q}}_\parallel)A_s(\boldsymbol{q}_\parallel)\right\} \\ &\quad \times \exp[i\boldsymbol{q}_\parallel \cdot \boldsymbol{x}_\parallel - \beta_0(q_\parallel)x_3], \end{aligned} \tag{2.1}$$

where

$$\boldsymbol{k}_\parallel = k_\parallel(\omega)(\cos\phi_0, \sin\phi_0, 0), \quad k_\parallel(\omega) = \frac{\omega}{c}\left[\frac{\epsilon(\omega)}{\epsilon(\omega)+1}\right]^{\frac{1}{2}}, \tag{2.2}$$

and $\phi_0$ is the azimuthal angle of incidence of the surface plasmon polariton, measured counterclockwise from the negative $x_1$ axis. The subscripts $p$ and $s$ denote the $p$- and $s$-polarized components of each of these fields with respect to the plane of incidence, defined by the vectors $\hat{\mathbf{k}}_\parallel$ and $\hat{\mathbf{x}}_3$, and the plane of scattering, defined by the vectors $\hat{\mathbf{q}}_\parallel$ and $\hat{\mathbf{x}}_3$, respectively.

The function $\beta_0(q_\parallel)$ appearing in Eq. 2.1 is defined by

$$\beta_0(q_\parallel) = [q_\parallel^2 - (\omega/c)^2]^{\frac{1}{2}}, \quad Re\beta_0(q_\parallel) > 0, \quad Im\beta_0(q_\parallel) < 0. \tag{2.3}$$

The function $\beta_0(k_\parallel) = (\omega/c)\{-1/[\epsilon(\omega)+1]\}^{\frac{1}{2}}$ is real and positive because $\epsilon(\omega)$ is real and negative.

We can write a similar expression for the electric field in the region $x_3 < \zeta(\boldsymbol{x}_\parallel)_{\min}$, and use it with Eq. 2.1 in satisfying the boundary conditions at the surface $x_3 = \zeta(\boldsymbol{x}_\parallel)$. However, it has been shown in [25] that the field in the medium can be eliminated from the problem. The amplitudes $A_{p,s}(\boldsymbol{q}_\parallel)$ then satisfy a matrix integral equation, called the reduced Rayleigh equation, which can be written in the form

$$\begin{aligned} &\frac{1}{1-\epsilon(\omega)}\begin{bmatrix} \epsilon(\omega)\beta_0(p_\parallel)+\beta(p_\parallel) & 0 \\ 0 & \beta_0(p_\parallel)+\beta(p_\parallel) \end{bmatrix}\begin{bmatrix} A_p(\boldsymbol{p}_\parallel) \\ A_s(\boldsymbol{p}_\parallel) \end{bmatrix} \\ &+\int \frac{d^2q_\parallel}{(2\pi)^2} J(\beta(p_\parallel) - \beta_0(q_\parallel)|\boldsymbol{p}_\parallel - \boldsymbol{q}_\parallel) \\ &\times \begin{bmatrix} p_\parallel q_\parallel - \beta(p_\parallel)\hat{\mathbf{p}}_\parallel \cdot \hat{\mathbf{q}}_\parallel \beta_0(q_\parallel) & -i(\omega/c)\beta(p_\parallel)(\hat{\mathbf{p}}_\parallel \times \hat{\mathbf{q}}_\parallel)_3 \\ i(\omega/c)(\hat{\mathbf{p}}_\parallel \times \hat{\mathbf{q}}_\parallel)_3\beta_0(q_\parallel) & (\omega/c)^2\hat{\mathbf{p}}_\parallel \cdot \hat{\mathbf{q}}_\parallel \end{bmatrix}\begin{bmatrix} A_p(\boldsymbol{q}_\parallel) \\ A_s(\boldsymbol{q}_\parallel) \end{bmatrix} \\ &= -J(\beta(p_\parallel) - \beta_0(k_\parallel)|\boldsymbol{p}_\parallel - \boldsymbol{k}_\parallel)\begin{bmatrix} P_\parallel - \beta(p_\parallel)\hat{\mathbf{p}}_\parallel \cdot \hat{\mathbf{k}}_\parallel \beta_0(k_\parallel) \\ i(\omega/c)(\hat{\mathbf{p}}_\parallel \times \hat{\mathbf{k}}_\parallel)_3\beta_0(k_\parallel) \end{bmatrix}, \end{aligned} \tag{2.4}$$

where

$$J(\alpha|\boldsymbol{Q}_\parallel) = \int d^2x_\parallel e^{-i\boldsymbol{Q}_\parallel \cdot \boldsymbol{x}_\parallel}\frac{e^{\alpha\zeta(x_1)}-1}{\alpha}, \tag{2.5}$$

$$= 2\pi\delta(Q_2)F(\alpha|Q_1), \tag{2.6a}$$

with

$$F(\alpha|Q_1) = \int_{-\infty}^{\infty} dx_1 e^{-iQ_1x_1}\frac{e^{\alpha\zeta(x_1)}-1}{\alpha}. \tag{2.6b}$$

The function $\beta(q_\parallel)$ is defined by

$$\beta(q_\parallel) = [q_\parallel^2 - \epsilon(\omega)(\omega/c)^2]^{\frac{1}{2}}, \quad Re\beta(q_\parallel) > 0, \quad Im\beta(q_\parallel) < 0. \tag{2.7}$$

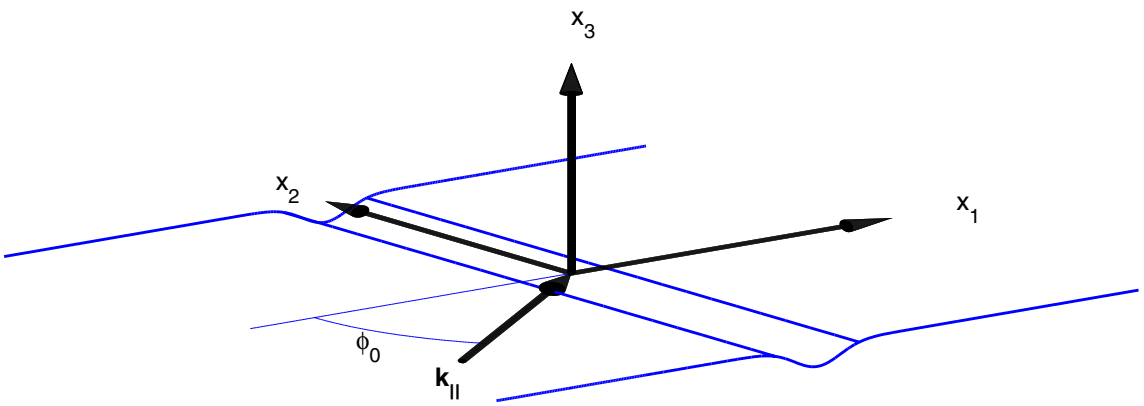


**Fig. 1** The schematic diagram of the studied system

The vanishing of the coefficient of $A_p(\boldsymbol{p}_\parallel)$ on the left-hand-side of Eq. 2.4 is the dispersion relation for surface plasmon polaritons at the planar interface between vacuum and a metal whose dielectric function is $\epsilon(\omega)$. This means that the coefficient $A_p(\boldsymbol{p}_\parallel)$ has a pole at $q_\parallel = k_\parallel$. It is preferable to solve integral equations for smoothly varying functions than for functions with singularities. Thus, we wish to remove the singularity from the function we solve for. At the same time, the infinitesimal translational invariance of our system in the $x_2$ direction has the consequence that the two components of the two-dimensional wave vectors appearing in this problem is conserved in the scattering. We deal with both of these points by introducing new unknown amplitudes $c_{p,s}(p_1)$ by

$$A_p(\boldsymbol{p}_\parallel) = 2\pi\delta(p_2 - k_2)\frac{c_p(p_1)}{\epsilon(\omega)\beta_0(p_\parallel) + \beta(p_\parallel)} \tag{2.8a}$$

and

$$A_s(\boldsymbol{p}_\parallel) = 2\pi\delta(p_2 - k_2)\frac{c_s(p_1)}{\beta_0(p_\parallel) + \beta(p_\parallel)}. \tag{2.8b}$$

When these expressions are substituted into Eq. 2.4, we obtain the equations satisfied by $c_{p,s}(p_1)$. We write them in the form

$$\begin{aligned}\begin{bmatrix} c_p(p_1) \\ c_s(p_1) \end{bmatrix} &= (\epsilon(\omega) - 1)F(\beta(p_\parallel) - \beta_0(k_\parallel)|p_1 - k_1)\begin{bmatrix} p_\parallel k_\parallel - \beta(p_\parallel)\hat{\mathbf{p}}_\parallel \cdot \hat{\mathbf{k}}_\parallel \beta_0(k_\parallel) \\ i(\omega/c)(\hat{\mathbf{p}}_\parallel \times \hat{\mathbf{k}}_\parallel)_3 \beta_0(k_\parallel) \end{bmatrix} \\ &+(\epsilon(\omega) - 1)\int_{-\infty}^{\infty}\frac{dq_1}{2\pi}F(\beta(p_\parallel) - \beta_0(q_\parallel)|p_1 - q_1) \\ &\times \begin{bmatrix} \frac{p_\parallel q_\parallel - \beta(p_\parallel)\hat{\mathbf{p}}_\parallel\cdot\hat{\mathbf{q}}_\parallel\beta_0(q_\parallel)}{\epsilon(\omega)\beta_0(q_\parallel)+\beta(q_\parallel)} & -\frac{i(\omega/c)\beta(p_\parallel)(\hat{\mathbf{p}}_\parallel\times\hat{\mathbf{q}}_\parallel)_3}{\beta_0(q_\parallel)+\beta(q_\parallel)} \\ \frac{i(\omega/c)(\hat{\mathbf{p}}_\parallel\times\hat{\mathbf{q}}_\parallel)_3\beta_0(q_\parallel)}{\epsilon(\omega)\beta_0(q_\parallel)+\beta(q_\parallel)} & \frac{(\omega/c)^2\hat{\mathbf{p}}_\parallel\cdot\hat{\mathbf{q}}_\parallel}{\beta_0(q_\parallel)+\beta(q_\parallel)} \end{bmatrix}\begin{bmatrix} c_p(q_1) \\ c_s(q_1) \end{bmatrix}. \end{aligned} \tag{2.9}$$

Although, to simplify the notation, we have written this equation in terms of the vectors $\boldsymbol{p}_\parallel$ and $\boldsymbol{q}_\parallel$, we emphasize that the two components of each vector is $k_2(\omega)$, so that

$$\boldsymbol{p}_\parallel = (p_1, k_2, 0), \quad p_\parallel = (p_1^2 + k_2^2)^{\frac{1}{2}}, \quad \hat{\mathbf{p}}_\parallel = \frac{(p_1, k_2, 0)}{(p_1^2 + k_2^2)^{\frac{1}{2}}}, \tag{2.10a}$$

and

$$\boldsymbol{q}_\parallel = (q_1, k_2, 0), \quad q_\parallel = (q_1^2 + k_2^2)^{\frac{1}{2}}, \quad \hat{\mathbf{q}}_\parallel = \frac{(q_1, k_2, 0)}{(q_1^2 + k_2^2)^{\frac{1}{2}}}. \tag{2.10b}$$

Equation 2.9 is the equation we have to solve. We will do so numerically.

## The Reflection, Transmission, and Radiation Coefficients

To determine the reflectivity and transmissivity of the surface plasmon polariton, and the out-of-plane scattering coefficient, we need the total time-averaged incident, reflected, and transmitted fluxes of the energy of the surface plasmon polariton and of the volume electromagnetic field scattered into the vacuum.

The electric and magnetic fields of the incident surface plasmon polariton in the vacuum region $x_3 > \zeta(x_1)$ are

$$\begin{aligned}\boldsymbol{E}^{>}(\mathbf{x}|\omega)_{\rm inc} &= \frac{c}{\omega}(i\hat{k}_1\beta_0(k_\parallel), i\hat{k}_2\beta_0(k_\parallel), \\ &- k_\parallel)\exp[i\boldsymbol{k}_\parallel\cdot\boldsymbol{x}_\parallel - \beta_0(k_\parallel)x_3] \end{aligned} \tag{3.1a}$$

$$\boldsymbol{H}^{>}(\mathbf{x}|\omega)_{\rm inc} = (-\hat{k}_2, \hat{k}_1, 0)\exp[i\boldsymbol{k}_\parallel\cdot\boldsymbol{x}_\parallel - \beta_0(k_\parallel)x_3], \tag{3.1b}$$

while in the region of the metal $x_3 < \zeta(x_1)$, they are

$$\begin{aligned}\boldsymbol{E}^{<}(\mathbf{x}|\omega)_{\rm inc} &= \frac{c}{\omega}\left(i\hat{k}_1\beta_0(k_\parallel), i\hat{k}_2\beta_0(k_\parallel), \frac{\beta_0(k_\parallel)}{\beta(k_\parallel)}k_\parallel\right) \\ &\exp[i\boldsymbol{k}_\parallel\cdot\boldsymbol{x}_\parallel + \beta(k_\parallel)x_3] \end{aligned} \tag{3.2a}$$

$$\boldsymbol{H}^{<}(\mathbf{x}|\omega)_{\rm inc} = (-\hat{k}_2, \hat{k}_1, 0)\exp[i\boldsymbol{k}_\parallel\cdot\boldsymbol{x}_\parallel + \beta(k_\parallel)x_3]. \tag{3.2b}$$

Consequently, the time-averaged Poynting vector for the surface plasmon polariton in the vacuum region is

$$\begin{aligned}\langle\boldsymbol{S}^{>}(\mathbf{x}|\omega)\rangle_{\rm inc} &= \frac{c^2}{8\pi\omega}Re(k_1, k_2, i\beta_0(k_\parallel))\exp[-2\beta_0(k_\parallel)x_3] \\ &= \frac{c^2}{8\pi\omega}\boldsymbol{k}_\parallel\exp[-2\beta_0(k_\parallel)x_3]. \end{aligned} \tag{3.3}$$

Thus the magnitude of the total time-averaged incident flux in the vacuum per unit width of the field is

$$P^{>}_{\rm inc} = \frac{c^2}{8\pi\omega}\frac{k_\parallel}{2\beta_0(k_\parallel)}. \tag{3.4}$$

Similarly, the total time-averaged Poynting vector for the surface plasmon polariton in the metal is

$$\begin{aligned}\langle \boldsymbol{S}^{<}(\mathbf{x}|\omega)\rangle_{\text{inc}} &= -\frac{c^2}{8\pi\omega}\frac{\beta_0(k_\parallel)}{\beta(k_\parallel)} Re(k_1, k_2, -i\beta(k_\parallel)) \\ &\quad \exp[2\beta(k_\parallel)x_3] \\ &= \frac{c^2}{8\pi\omega\epsilon(\omega)}\boldsymbol{k}_\parallel \exp[2\beta(k_\parallel)x_3]. \end{aligned} \tag{3.5}$$

The magnitude of the total time-averaged incident flux in the metal per unit width of the field is therefore

$$P^{<}_{\text{inc}} = \frac{c^2}{8\pi\omega\epsilon(\omega)}\frac{k_\parallel}{2\beta(k_\parallel)}. \tag{3.6}$$

Thus, the total incident flux is

$$\begin{aligned} P_{\text{inc}} = P^{>}_{\text{inc}} + P^{<}_{\text{inc}} &= \frac{c^2}{16\pi\omega}k_\parallel\left(\frac{1}{\beta_0(k_\parallel)} + \frac{1}{\epsilon(\omega)\beta(k_\parallel)}\right) \\ &= \frac{c^2}{16\pi\omega}\frac{k_\parallel}{\beta_0(k_\parallel)}\left(1 - \frac{1}{\epsilon^2(\omega)}\right). \end{aligned} \tag{3.7}$$

We now turn to the reflected and transmitted surface plasmon polaritons. As a surface plasmon polariton is $p$-polarized, we consider the contribution to the scattered electric field in the vacuum from the $p$-polarized waves which, in view of Eqs. 2.1 and 2.8a, becomes

$$\begin{aligned}\boldsymbol{E}^{>}(\mathbf{x}|\omega)_{sc,p} = \int_{-\infty}^{\infty} \frac{dq_1}{2\pi}\frac{c}{\omega}[i\beta_0(q_\parallel)\hat{\mathbf{q}}_\parallel - q_\parallel\hat{\mathbf{x}}_3]\frac{c_p(q_1)}{\epsilon(\omega)\beta_0(q_\parallel) + \beta(q_\parallel)} \\ \times \exp[i\boldsymbol{q}_\parallel\cdot\boldsymbol{x}_\parallel - \beta_0(q_\parallel)x_3], \end{aligned} \tag{3.8}$$

where it should be understood that $q_2 = k_2$. The contribution to this expression from the surface plasmon polariton is given by the residues at the poles of the integrand occurring at $q_1 = \pm k_1$. The manner in which this calculation is carried out is described in [26], and we present only the results here.

Thus, for the scattered fields in the vacuum we have

$$\begin{aligned}\boldsymbol{E}^{>}(\mathbf{x}|\omega)_{sc,spp} &= it(\omega)\frac{c}{\omega}[i\beta_0(k_\parallel)\hat{k}_1, i\beta_0(k_\parallel)\hat{k}_2, -k_\parallel] \\ &\quad \times\exp[ik_1x_1 + ik_2x_2 - \beta_0(k_\parallel)x_3] \quad x_1 > 0 \end{aligned} \tag{3.9a}$$

$$\begin{aligned}&= ir(\omega)\frac{c}{\omega}[-i\beta_0(k_\parallel)\hat{k}_1, i\beta_0(k_\parallel)\hat{k}_2, -k_\parallel] \\ &\times \exp[-ik_1x_1 + ik_2x_2 - \beta_0(k_\parallel)x_3] \quad x_1 < 0 \end{aligned} \tag{3.9b}$$

$$\begin{aligned}\boldsymbol{H}^{>}(\mathbf{x}|\omega)_{sc,spp} &= it(\omega)(-\hat{k}_2, \hat{k}_1, 0) \\ &\quad \times \exp[ik_1x_1 + ik_2x_2 - \beta_0(k_\parallel)x_3] \quad x_1 > 0 \end{aligned} \tag{3.10a}$$

$$\begin{aligned}&= ir(\omega)(-\hat{k}_2, -\hat{k}_1, 0) \\ &\times \exp[-ik_1x_1 + ik_2x_2 - \beta_0(k_\parallel)x_3] \quad x_1 < 0, \end{aligned} \tag{3.10b}$$

where

$$t(\omega) = \frac{\epsilon(\omega)}{\epsilon^2(\omega) - 1}\frac{\beta_0(k_\parallel)}{k_1}c_p(k_1) \tag{3.11a}$$

$$r(\omega) = \frac{\epsilon(\omega)}{\epsilon^2(\omega) - 1}\frac{\beta_0(k_\parallel)}{k_1}c_p(-k_1). \tag{3.11b}$$

Similarly, for the scattered fields in the metal we have

$$\begin{aligned}\boldsymbol{E}^{<}(\mathbf{x}|\omega)_{sc,spp} &= it(\omega)\frac{c}{\omega}\left[i\beta_0(k_\parallel)\hat{k}_1, i\beta_0(k_\parallel)\hat{k}_2, -\frac{k_\parallel}{\epsilon(\omega)}\right] \\ &\quad \times \exp[ik_1x_1 + ik_2x_2 + \beta(k_\parallel)x_3] \quad x_1 > 0 \end{aligned} \tag{3.12a}$$

$$\begin{aligned}&= ir(\omega)\frac{c}{\omega}\left[-i\beta_0(k_\parallel)\hat{k}_1, i\beta_0(k_\parallel)\hat{k}_2, -\frac{k_\parallel}{\epsilon(\omega)}\right] \\ &\times \exp[-ik_1x_1 + ik_2x_2 + \beta(k_\parallel)x_3] \quad x_1 < 0 \end{aligned} \tag{3.12b}$$

$$\begin{aligned}\boldsymbol{H}^{<}(\mathbf{x}|\omega)_{sc,spp} &= it(\omega)(-\hat{k}_2, \hat{k}_1, 0) \\ &\quad \times \exp[ik_1x_1 + ik_2x_2 + \beta(k_\parallel)x_3] \quad x_1 > 0 \end{aligned} \tag{3.13a}$$

$$\begin{aligned}&= ir(\omega)(-\hat{k}_2, -\hat{k}_1, 0) \\ &\times \exp[-ik_1x_1 + ik_2x_2 + \beta(k_\parallel)x_3] \quad x_1 < 0. \end{aligned} \tag{3.13b}$$

The time-averaged Poynting vector of the reflected plasmon polariton in the vacuum region is therefore

$$\langle \boldsymbol{S}^{>}(\mathbf{x}|\omega)\rangle_{\text{ref}} = \frac{c^2}{8\pi\omega}|r(\omega)|^2(-k_1, k_2, 0)\exp[-2\beta_0(k_\parallel)x_3]. \tag{3.14}$$

Thus the total time-averaged reflected flux per unit width of the field is

$$\boldsymbol{P}^{>}_{\text{ref}} = \frac{c^2}{8\pi\omega}|r(\omega)|^2\frac{(-k_1, k_2, 0)}{2\beta_0(k_\parallel)}. \tag{3.15}$$

Similarly, the time-averaged Poynting vector of the reflected plasmon polariton in the metal is

$$\langle \boldsymbol{S}^{<}(\mathbf{x}|\omega)\rangle_{\text{ref}} = \frac{c^2}{8\pi\omega\epsilon(\omega)}|r(\omega)|^2(-k_1, k_2, 0)\exp[2\beta(k_\parallel)x_3]. \tag{3.16}$$

Therefore the total time-averaged reflected flux per unit width of the field in the metal is

$$\begin{aligned}\boldsymbol{P}^{<}_{\text{ref}} &= \frac{c^2}{8\pi\omega\epsilon(\omega)}|r(\omega)|^2\frac{(-k_1, k_2, 0)}{2\beta(k_\parallel)} \\ &= \frac{c^2}{8\pi\omega\epsilon(\omega)}|r(\omega)|^2\frac{(-k_1, k_2, 0)}{2\beta_0(k_\parallel)}\frac{\beta_0(k_\parallel)}{\beta(k_\parallel)} \\ &= -\frac{c^2}{8\pi\omega}|r(\omega)|^2\frac{(-k_1, k_2, 0)}{2\beta(k_\parallel)}\frac{1}{\epsilon^2(\omega)}. \end{aligned} \tag{3.17}$$

The total flux of the reflected surface plasmon polariton is therefore

$$\begin{aligned}\boldsymbol{P}_{\text{ref}} &= \boldsymbol{P}^{>}_{\text{ref}} + \boldsymbol{P}^{<}_{\text{ref}} \\ &= \frac{c^2}{8\pi\omega}|r(\omega)|^2 \frac{(-k_1, k_2, 0)}{2\beta_0(k_\parallel)}\left(1 - \frac{1}{\epsilon^2(\omega)}\right). \end{aligned} \tag{3.18}$$

The magnitude of this flux is

$$P_{\text{ref}} = \frac{c^2}{8\pi\omega}|r(\omega)|^2 \frac{k_\parallel}{2\beta_0(k_\parallel)}\left(1 - \frac{1}{\epsilon^2(\omega)}\right). \tag{3.19}$$

Thus, the reflectivity of the surface plasmon polariton is

$$R(\omega) = \frac{P_{\text{ref}}}{P_{\text{inc}}} = |r(\omega)|^2. \tag{3.20}$$

Turning now to the surface plasmon polariton transmission coefficient, we see from Eqs. 3.1, 3.2, 3.9a, 3.10a, 3.12a, and 3.13a that the total electric and magnetic fields of the surface plasmon polariton in the region $x_1 > 0$ in the vacuum and the metal can be written

$$\begin{aligned}\boldsymbol{E}^{>}(\mathbf{x}|\omega)_{\text{tr, spp}} &= (1 + it(\omega))\frac{c}{\omega}[i\beta_0(k_\parallel)\hat{k}_1, i\beta_0(k_\parallel)\hat{k}_2, -k_\parallel] \\ &\quad \times \exp[ik_1x_1 + ik_2x_2 - \beta_0(k_\parallel)x_3] \end{aligned} \tag{3.21a}$$

$$\begin{aligned}\boldsymbol{H}^{>}(\mathbf{x}|\omega)_{\text{tr, spp}} &= (1 + it(\omega))(-\hat{k}_2, \hat{k}_1, 0) \\ &\quad \times \exp[ik_1x_1 + ik_2x_2 - \beta_0(k_\parallel)x_3], \end{aligned} \tag{3.21b}$$

and

$$\begin{aligned}\boldsymbol{E}^{<}(\mathbf{x}|\omega)_{\text{tr, spp}} &= (1 + it(\omega))\frac{c}{\omega}\left[i\beta_0(k_\parallel)\hat{k}_1, i\beta_0(k_\parallel)\hat{k}_2, -\frac{k_\parallel}{\epsilon(\omega)}\right] \\ &\quad \times \exp[ik_1x_1 + ik_2x_2 + \beta(k_\parallel)x_3] \end{aligned} \tag{3.22a}$$

$$\begin{aligned}\boldsymbol{H}^{<}(\mathbf{x}|\omega)_{\text{tr, spp}} &= (1 + it(\omega))(-\hat{k}_2, \hat{k}_1, 0) \\ &\quad \times \exp[ik_1x_1 + ik_2x_2 + \beta(k_\parallel)x_3]. \end{aligned} \tag{3.22b}$$

The first term on the right-hand side of each of these expressions arises from the incident field, which is present in the region $x_1 > 0$ even in the absence of the defect.

The time-averaged Poynting vector for the transmitted surface plasmon polariton in the vacuum is then given by

$$\begin{aligned}\langle \boldsymbol{S}^{>}(\mathbf{x}|\omega)\rangle_{\text{tr}} &= \frac{c^2}{8\pi\omega}|1 + it(\omega)|^2 Re(k_1, k_2, i\beta_0(k_\parallel)) \\ &\quad \exp[-2\beta_0(k_\parallel)x_3] \\ &= \frac{c^2}{8\pi\omega}|1 + it(\omega)|^2(k_1, k_2, 0) \\ &\quad \exp[-2\beta_0(k_\parallel)x_3]. \end{aligned} \tag{3.23}$$

Thus the total time-averaged transmitted flux per unit width of the field is

$$\boldsymbol{P}^{>}_{\text{tr}} = \frac{c^2}{8\pi\omega}|1 + it(\omega)|^2 \frac{\boldsymbol{k}_\parallel}{2\beta_0(k_\parallel)}. \tag{3.24}$$

The time-averaged Poynting vector of the transmitted surface plasmon polariton in the metal is

$$\begin{aligned}\langle \boldsymbol{S}^{<}(\mathbf{x}|\omega)\rangle_{\text{tr}} &= \frac{c^2}{8\pi\omega}|1 + it(\omega)|^2 \\ &\quad Re\left(\frac{k_1}{\epsilon(\omega)}, \frac{k_2}{\epsilon(\omega)}, i\beta_0(k_\parallel)\right)\exp[2\beta(k_\parallel)x_3] \\ &= \frac{c^2}{8\pi\omega\epsilon(\omega)}|1 + it(\omega)|^2(k_1, k_2, 0) \\ &\quad \exp[2\beta(k_\parallel)x_3]. \end{aligned} \tag{3.25}$$

Therefore, the total time-averaged transmitted flux per unit width of the field in the metal is

$$\boldsymbol{P}^{<}_{\text{tr}} = \frac{c^2}{8\pi\omega\epsilon(\omega)}|1 + it(\omega)|^2 \frac{\boldsymbol{k}_\parallel}{2\beta(k_\parallel)}. \tag{3.26}$$

The total flux of the transmitted surface plasmon polariton is therefore

$$\begin{aligned}\boldsymbol{P}_{\text{tr}} &= \frac{c^2}{8\pi\omega}|1 + it(\omega)|^2 \boldsymbol{k}_\parallel \left(\frac{1}{2\beta_0(k_\parallel)} + \frac{1}{2\epsilon(\omega)\beta(k_\parallel)}\right) \\ &= \frac{c^2}{8\pi\omega}|1 + it(\omega)|^2 \frac{\boldsymbol{k}_\parallel}{2\beta_0(k_\parallel)}\left(1 - \frac{1}{\epsilon^2(\omega)}\right). \end{aligned} \tag{3.27}$$

The magnitude of this flux is

$$P_{\text{tr}} = \frac{c^2}{8\pi\omega}|1 + it(\omega)|^2 \frac{k_\parallel}{2\beta_0(k_\parallel)}\left(1 - \frac{1}{\epsilon^2(\omega)}\right). \tag{3.28}$$

Consequently the transmissivity of the surface plasmon polariton is

$$T(\omega) = \frac{P_{\text{tr}}}{P_{\text{inc}}} = |1 + it(\omega)|^2. \tag{3.29}$$

To obtain the out-of-plane scattering coefficient we need the three-component of the Poynting vector of the electromagnetic field radiated into the vacuum region. This field contains both $p$- and $s$- polarized components. Its electric field, the integral term on the right-hand side of Eq. 2.1, can be written in the following form, which is particularly useful for calculating the radiated power:

$$\begin{aligned}\boldsymbol{E}^{>}(\mathbf{x}|\omega)_{sc} &= i\int_{-\infty}^{\infty}\frac{dq_1}{2\pi}\exp[i\boldsymbol{q}_\parallel\cdot\boldsymbol{x}_\parallel + i\alpha_0(q_\parallel)x_3] \\ &\quad \times\left[\frac{(c/\omega)[\alpha_0(q_\parallel)\hat{\mathbf{q}}_\parallel - q_\parallel\hat{\mathbf{x}}_3]}{\epsilon(\omega)\alpha_0(q_\parallel) + \alpha(q_\parallel)}c_p(q_1)\right. \\ &\quad \left. + \frac{(\hat{\mathbf{x}}_3\times\hat{\mathbf{q}}_\parallel)}{\alpha_0(q_\parallel) + \alpha(q_\parallel)}c_s(q_1)\right]. \end{aligned} \tag{3.30}$$

In writing this equation we have introduced the functions $\alpha_0(q_\parallel)$ and $\alpha(q_\parallel)$ through the relations

$$\beta_0(q_\parallel) = -i\alpha_0(q_\parallel), \quad \beta(q_\parallel) = -i\alpha(q_\parallel), \tag{3.31}$$

so that

$$\alpha_0(q_\parallel) = [(\omega/c)^2 - q_\parallel^2]^{\frac{1}{2}}, \quad Re\alpha_0(q_\parallel) > 0, \quad Im\alpha_0(q_\parallel) > 0 \tag{3.32a}$$

$$\alpha(q_\parallel) = [\epsilon(\omega)(\omega/c)^2 - q_\parallel^2]^{\frac{1}{2}}, \quad Re\alpha(q_\parallel) > 0, \quad Im\alpha(q_\parallel) > 0. \tag{3.32b}$$

It should be kept in mind that in these equations $q_2 = k_2$. The magnetic field radiated into the vacuum is then given by

$$\boldsymbol{H}^{>}(\mathbf{x}|\omega)_{\rm sc} = i\int_{-\infty}^{\infty}\frac{dq_1}{2\pi}\exp[i\boldsymbol{q}_\parallel\cdot\boldsymbol{x}_\parallel + i\alpha_0(q_\parallel)x_3] \times\left[\frac{(\hat{\mathbf{x}}_3\times\hat{\mathbf{q}}_\parallel)}{\epsilon(\omega)\alpha_0(q_\parallel)+\alpha(q_\parallel)}c_p(q_1) - \frac{(c/\omega)[\alpha_0(q_\parallel)\hat{\mathbf{q}}_\parallel - q_\parallel\hat{\mathbf{x}}_3]}{\alpha_0(q_\parallel)+\alpha(q_\parallel)}c_s(q_1)\right]. \tag{3.33}$$

The three-component of the total time-averaged scattered flux is then given by

$$\begin{aligned}P_{\rm sc}^{>} &= \int_{-\frac{L_1}{2}}^{\frac{L_1}{2}}dx_1\int_{-\frac{L_2}{2}}^{\frac{L_2}{2}}dx_2\langle S^{>}(\mathbf{x}|\omega)_3\rangle_{\rm sc}\\ &= \frac{c}{8\pi}Re\int_{-\frac{L_1}{2}}^{\frac{L_1}{2}}dx_1\int_{-\frac{L_2}{2}}^{\frac{L_2}{2}}dx_2\int_{-\infty}^{\infty}\frac{dq_1}{2\pi}\int_{-\infty}^{\infty}\frac{dq_1'}{2\pi}\\ &\times\exp[i(\boldsymbol{q}_\parallel-\boldsymbol{q}_\parallel')\cdot\boldsymbol{x}_\parallel + i(\alpha_0(q_\parallel)-\alpha_0^*(q_\parallel'))x_3]\\ &\times\left[\frac{(\hat{\boldsymbol{e}}_p(\boldsymbol{q}_\parallel)\times\hat{\boldsymbol{e}}_s^*(\boldsymbol{q}_\parallel'))_3}{d_p(q_\parallel)d_p^*(q_\parallel')}c_p(q_1)c_p^*(q_1')\right.\\ &-\frac{(\hat{\boldsymbol{e}_p}(\boldsymbol{q}_\parallel)\times\hat{\boldsymbol{e}_p}^*(\boldsymbol{q}_\parallel'))_3}{d_p(q_\parallel)d_s^*(q')}c_p(q_1)c_s^*(q_1')\\ &+\frac{(\hat{\boldsymbol{e}}_s(\boldsymbol{q}_\parallel)\times\hat{\boldsymbol{e}}_s^*(\boldsymbol{q}_\parallel'))_3}{d_s(q_\parallel)d_p^*(q_\parallel')}c_s(q_1)c_p^*(q_1')\\ &\left.-\frac{(\hat{\boldsymbol{e}}_s(\boldsymbol{q}_\parallel)\times\hat{\boldsymbol{e}}_p^*(\boldsymbol{q}_\parallel'))_3}{d_s(q_\parallel)d_s^*(q_\parallel')}c_s(q_1)c_s^*(q_1')\right],\end{aligned} \tag{3.34}$$

where $L_1$ and $L_2$ are the lengths of the surface along the $x_1$ and $x_2$ axes, respectively. In writing Eq. 3.34, we have introduced the orthogonal unit vectors $\hat{\boldsymbol{e}}_p(\boldsymbol{q}_\parallel)$ and $\hat{\boldsymbol{e}}_s(\boldsymbol{q}_\parallel)$ that are defined by

$$\hat{\boldsymbol{e}}_p(\boldsymbol{q}_\parallel) = \frac{c}{\omega}[\alpha_0(q_\parallel)\hat{\mathbf{q}}_\parallel - q_\parallel\hat{\mathbf{x}}_3], \quad \hat{\boldsymbol{e}}_s(\boldsymbol{q}_\parallel) = (\hat{\mathbf{x}}_3\times\hat{\mathbf{q}}_\parallel), \tag{3.35}$$

and the functions

$$d_p(q_\parallel) = \epsilon(\omega)\alpha_0(q_\parallel)+\alpha(q_\parallel), \quad d_s(q_\parallel) = \alpha_0(q_\parallel)+\alpha(q_\parallel). \tag{3.36}$$

After the integrations over $x_1$ and $x_2$ are carried out, Eq. 3.34 becomes

$$P_{\rm sc}^{>} = L_2\frac{c^2}{8\pi\omega}\int_{-\infty}^{\infty}\frac{dq_1}{2\pi}\exp[-2Im\alpha_0(q_\parallel)x_3] \times Re\left[\alpha_0(q_\parallel)\frac{|c_p(q_1)|^2}{|d_p(q_\parallel)|^2}+\alpha_0^*(q_\parallel)\frac{|c_s(q_1)|^2}{|d_s(q_\parallel)|^2}\right], \tag{3.37}$$

where $L_2$, the length of the surface along the $x_2$ axis, is assumed to equal the width of the incident surface plasmon polariton in the direction perpendicular to its direction of propagation. The function $\alpha_0(q_\parallel)$ is purely imaginary for $q_\parallel > (\omega/c)$, so that we finally obtain

$$P_{\rm sc}^{>} = L_2\frac{c^2}{16\pi^2\omega}\int_{-\sqrt{(\omega/c)^2-k_2^2}}^{\sqrt{(\omega/c)^2-k_2^2}} dq_1\alpha_0(q_\parallel)\left[\frac{|c_p(q_1)|^2}{|d_p(q_\parallel)|^2}+\frac{|c_s(q_1)|^2}{|d_s(q_\parallel)|^2}\right]. \tag{3.38}$$

Normalized by the incident flux, this function yields the out-of-plane scattering coefficient $S(\omega)$,

$$S(\omega) = \frac{1}{\pi}\frac{|\epsilon(\omega)|^{3/2}}{\epsilon^2(\omega)-1}\int_{-\sqrt{(\omega/c)^2-k_2^2}}^{\sqrt{(\omega/c)^2-k_2^2}} dq_1\alpha_0(q_\parallel)\left[\frac{|c_p(q_1)|^2}{|d_p(q_\parallel)|^2}+\frac{|c_s(q_1)|^2}{|d_s(q_\parallel)|^2}\right]. \tag{3.39}$$

To obtain the angular distribution of the intensity of the field scattered into the vacuum, we note that in terms of the polar ($\theta_s$) and azimuthal ($\phi_s$) angles of scattering we have

$$q_1 = \frac{\omega}{c}\sin\theta_s\cos\phi_s \tag{3.40}$$

$$q_2 = \frac{\omega}{c}\sin\theta_s\sin\phi_s = k_2 = \frac{\omega}{c}n(\omega)\sin\phi_0, \tag{3.41}$$

where $0 \le \theta_s \le \pi/2$, and $-\pi \le \phi_s \le \pi$, while $n(\omega) = [\epsilon(\omega)/(\epsilon(\omega)+1)]^{\frac{1}{2}}$. From Eqs. 3.40–3.41 we find that

$$q_1 = n(\omega)\frac{\omega}{c}\sin\phi_0\cot\phi_s \tag{3.42}$$

$$\alpha_0(q_\parallel) = \frac{\omega}{c}\left[1-n^2(\omega)\frac{\sin^2\phi_0}{\sin^2\phi_s}\right]^{\frac{1}{2}}. \tag{3.43}$$

As we are interested in the field scattered into the vacuum region and not in grazing angle scattering, we have to restrict $\theta_s$ to be smaller than $\pi/2$. For what range of the azimuthal scattering angle $\phi_s$ is this condition satisfied? We see from Eq. 3.41 that when $\theta_s = \pi/2$, $\sin\phi_s = n(\omega)\sin\phi_0$. This equation is satisfied for $\phi_s = \sin^{-1}(n(\omega)\sin\phi_0)$ and $\phi_s = \pi - \sin^{-1}(n(\omega)\sin\phi_0)$. Consequently, it is for $\phi_s$ between these values that $\theta_s$ is smaller than $\pi/2$. However,

we can say more about the angular range in the vacuum within which the scattered field exists.

Consider the vector from the origin to the point $(q, \theta_s, \phi_s)$ in spherical coordinates. Its representation in Cartesian coordinates is

$$\mathbf{q} = q(\sin\theta_s \cos\phi_s, \sin\theta_s \sin\phi_s, \cos\theta_s). \tag{3.44}$$

The angle $\alpha$ it makes with the $x_2$ axis is obtained from

$$\hat{\mathbf{q}} \cdot \hat{\mathbf{x}}_2 = \cos\alpha = \sin\theta_s \sin\phi_s. \tag{3.45}$$

If this vector is rotated about the $x_2$ axis with the angle $\alpha$ kept fixed, it generates a cone whose axis is the $x_2$ axis and whose interior angle is $2\alpha$. Thus, we see from Eq. 3.41 that the scattered field lies on the surface of a cone whose axis is the $x_2$ axis and whose angle $\alpha$ is defined by

$$\cos\alpha = n(\omega)\sin\phi_0. \tag{3.46}$$

This conclusion is compatible with the limits on the variation of $\phi_s$ within which $\theta_s < \pi/2$.

We now return to Eq. 3.39. From Eq. 3.42 we find that

$$dq_1 = -n(\omega)\frac{\omega}{c}\frac{\sin\phi_0}{\sin^2\phi_s}d\phi_s. \tag{3.47}$$

When $q_1 = [(\omega/c)^2 - k_2^2]^{\frac{1}{2}}$, we obtain from Eq. 3.41 that $\phi_s = \sin^{-1}(n(\omega)\sin\phi_0)$. When $q_1 = -[(\omega/c)^2 - k_2^2]^{\frac{1}{2}}$, we find that $\phi_s = \pi - \sin^{-1}(n(\omega)\sin\phi_0)$. These results, together with Eq. 3.43, transform Eq. 3.39 into

$$\begin{aligned} S(\omega) &= -\frac{1}{\pi}\left(\frac{\omega}{c}\right)^2 \frac{|\epsilon(\omega)|^{3/2}}{\epsilon^2(\omega)-1} n(\omega)\sin\phi_0 \\ &\times \int_{\pi-\gamma}^{\gamma} d\phi_s \frac{[\sin^2\phi_s - n^2(\omega)\sin^2\phi_0]^{\frac{1}{2}}}{|\sin\phi_s|^3}\left[\frac{|c_p(q_1)|^2}{|d_p(q_\parallel)|^2} + \frac{|c_s(q_1)|^2}{|d_s(q_\parallel)|^2}\right] \\ &= \frac{1}{\pi}\left(\frac{\omega}{c}\right)^2 \frac{\epsilon^2(\omega)}{(|\epsilon(\omega)|+1)(|\epsilon(\omega)|-1)^{3/2}}\sin\phi_0 \\ &\times \int_{\gamma}^{\pi-\gamma} d\phi_s \frac{[\sin^2\phi_s - \sin^2\gamma]^{\frac{1}{2}}}{|\sin\phi_s|^3}\left[\frac{|c_p(q_1)|^2}{|d_p(q_\parallel)|^2} + \frac{|c_s(q_1)|^2}{|d_s(q_\parallel)|^2}\right] \\ &\equiv \int_{\gamma}^{\pi-\gamma} d\phi_s S(\theta_s, \phi_s|\omega), \end{aligned} \tag{3.48}$$

where $\gamma = \sin^{-1}(n(\omega)\sin\phi_0) = (\pi/2) - \alpha$. Although we have written the integrand in Eq. 3.48 as a function of both $\theta_s$ and $\phi_s$, it should be kept in mind that in view of Eq. 3.41, $\theta_s$ is not independent of $\phi_s$. The fraction of the total time-averaged incident flux that is scattered into the angular region $(\phi_s, \phi_s + d\phi_s)$ in the vacuum region is therefore

$$\begin{aligned} S(\theta_s, \phi_s|\omega) &= \frac{1}{\pi}\left(\frac{\omega}{c}\right)^2 \frac{\epsilon^2(\omega)}{(|\epsilon(\omega)|+1)(|\epsilon(\omega)|-1)^{3/2}}\sin\phi_0 \\ &\times \frac{[\sin^2\phi_s - \sin^2\gamma]^{\frac{1}{2}}}{|\sin\phi_s|^3}\left[\frac{|c_p(q_1)|^2}{|d_p(q_\parallel)|^2} + \frac{|c_s(q_1)|^2}{|d_s(q_\parallel)|^2}\right], \end{aligned} \tag{3.49}$$

where $\gamma \le \phi_s \le \pi - \gamma$, and $\theta_s = \sin^{-1}(n(\omega)\sin\phi_0/\sin\phi_s)$.

### The Numerical Solution of Equation 2.9

In solving Eq. 2.9 numerically, we first replace the infinite region of integration by the finite region $(-Q, Q)$, where $Q$ is typically in the range $6(\omega/c) - 7(\omega/c)$. Integration over this region is then replaced by summation through the use of a numerical quadrature scheme, namely the extended midpoint rule [27]. Different integration mesh sizes are used in different regions of the $q_1$ axis, depending on the nature of the integrand in these regions. The poles in the kernel of the equation for $c_p(p_1)$ at $q_1 = \pm k_1(\omega)$, arising from the vanishing of the denominator in the factor $1/[\epsilon(\omega)\beta_0(q_\parallel) + \beta(q_\parallel)]$ are dealt with by giving $\epsilon(\omega)$ in only this denominator an infinitesimal positive imaginary part. It is convenient to choose the integration mesh in such a way that $\pm k_1(\omega)$ are among the values that $q_1$ takes. This simplifies the determination of $c_p(\pm k_1(\omega))$, in terms of which the surface plasmon polariton reflection $R(\omega)$ and transmission $T(\omega)$ coefficients are expressed. When the wave number $p_1$ is given the same discrete values that $q_1$ takes, a pair of coupled matrix equations is obtained for the values of $c_p(p_1)$ and $c_s(p_1)$ at these values of $q_1$. This system of equations is solved by a linear system equation solver algorithm [28]. A detailed description of this method of solution is presented in [13].

### Results

To illustrate the preceding results, we have calculated the reflection and transmission of a surface plasmon polariton incident obliquely on a ridge or groove on an otherwise planar silver surface, and its conversion into volume electromagnetic waves in the vacuum.

The dielectric function for silver was assumed to have the free electron form

$$\epsilon(\omega) = 1 - \frac{\omega_p^2}{\omega^2}, \tag{5.1}$$

with a value of the plasma frequency given by $\omega_p = 11.76 \times 10^{15}\mathrm{s}^{-1}$. This value was obtained from the value of the surface impedance $\xi = [\epsilon(\omega)]^{-\frac{1}{2}} = -0.227i$ at a wavelength $\lambda = 600$ nm [14].

In our illustrative example, the surface profile function $\zeta(x_1)$ is assumed to have the Gaussian form

$$\zeta(x_1) = A\exp(-x_1^2/R^2). \tag{5.2}$$

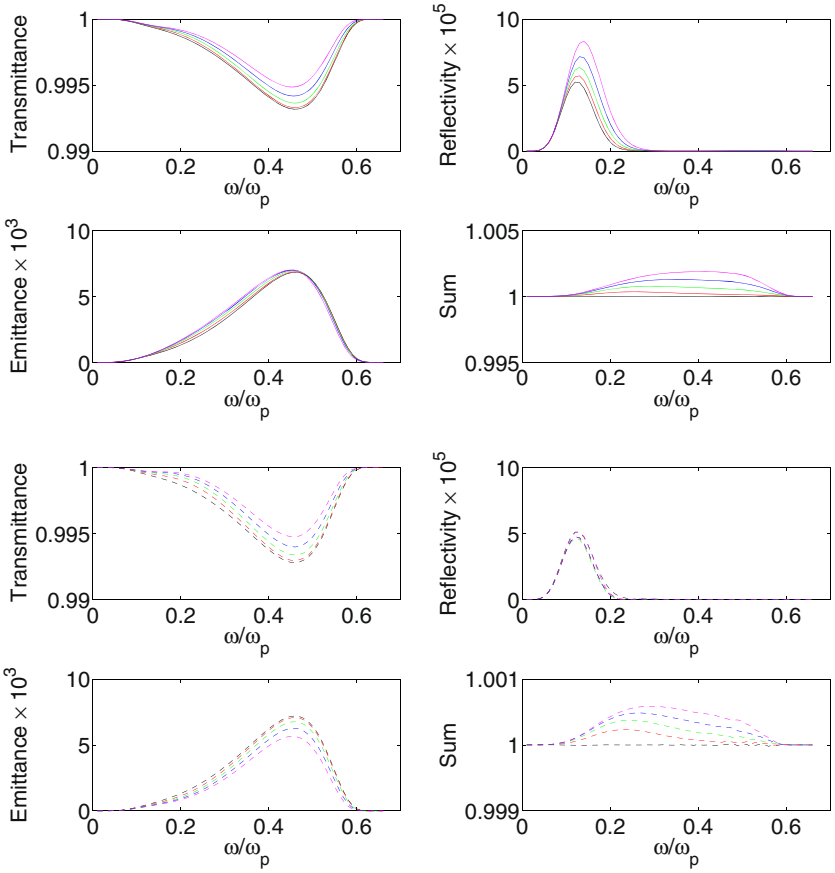


**Fig. 2** The frequency dependence of the transmittance, reflectance, and emittance, when a surface plasmon polariton is incident at an angle $\phi_0 = 0°$ (*black curves*), 5 ° (*red curves*), 10 ° (*green curves*), 15 ° (*blue curves*), and 20 ° (*magenta curves*) on a Gaussian surface defect, defined by Eq. 5.2, on an otherwise planar silver surface. The values of the parameters assumed in obtaining these results are $\omega_p = 11.76 \times 10^{15}$ s$^{-1}$, $R = 250$ nm, $A = 12$ nm (*solid curve*) and $A = -12$ nm (*dashed curve*)

It describes a ridge when $A$ is positive, and a groove when $A$ is negative. The function $F(\alpha|Q)$ corresponding to this profile function is

$$F(\alpha|Q) = \sqrt{\pi} R \sum_{n=1}^{\infty} \frac{\alpha^{n-1} A^n}{\sqrt{n} n!} \exp\left(-\frac{R^2 Q^2}{4n}\right). \tag{5.3}$$

The frequency dependence of the transmittance $T(\omega)$, the reflectance $R(\omega)$, and the out-of-plane scattering coefficient $S(\omega)$ has been calculated for the case where a surface plasmon polariton is incident on a groove or ridge at an angle $\phi_0$ from the normal to the defect. The defect is defined by Eq. 5.2. Its $1/e$ halfwidth $R$ is fixed at a value $R = 250$ nm, while its amplitude $A$ is given the values $A = \pm 12$ nm ($\phi_0 = 5, 10, 15, 20$ °), $A = \pm 24$ nm ($\phi_0 = 5, 10$ °), and $A = \pm 36$ nm ($\phi_0 = 2.5, 5$ °). These results are compared with those obtained when the surface plasmon polariton is incident normally on the defect ($\phi_0 = 0$ °). The spectral range within which these functions are calculated is $0 < \omega < \omega_p/\sqrt{2}$, i.e., the range within which a surface plasmon polariton exists at a vacuum-free electron metal interface.

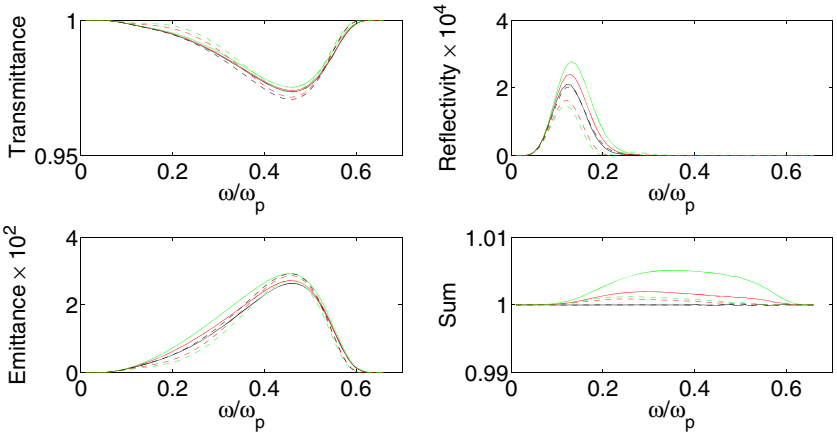


**Fig. 3** The same as Fig. 2, but for $\phi_0 = 0$ ° (*black curves*), 5 ° (*red curves*), 10 ° (*green curves*), and $|A| = 24$ nm

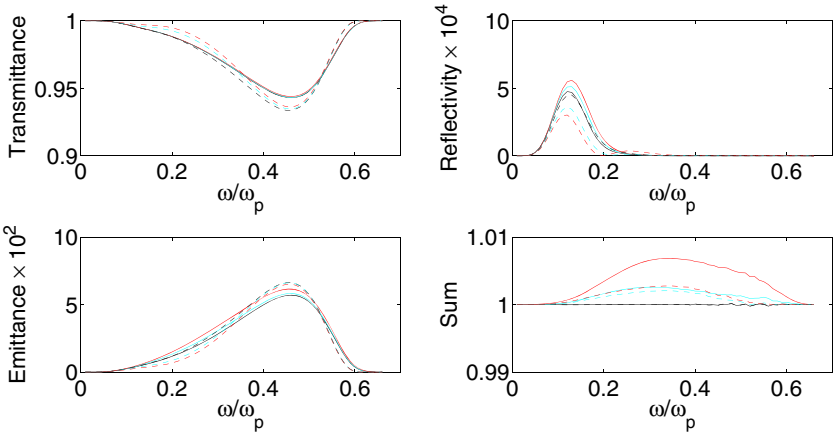


**Fig. 4** The same as Fig. 2, but for $\phi_0 = 0°$ (*black curves*), 2.5 ° (*cyan curves*), 5 ° (*red curves*), and $|A| = 36$ nm

In Fig. 2, we present plots of $T(\omega)$, $R(\omega)$, $S(\omega)$, and the sum $R(\omega) + S(\omega) + T(\omega)$ as functions of frequency for a defect defined by $A = \pm 12$ nm. The transmittance $T(\omega)$ has a single minimum for both a ridge and a groove, the emittance $S(\omega)$ has a single maximum for both surface profiles, as does the reflectance $R(\omega)$. We see from these results that the reflectance is smaller than the transmittance and emittance by factors of about 10,000 and 100, respectively. For normal incidence, the differences between the values of $T(\omega)$, $R(\omega)$, and $S(\omega)$ for a ridge and a groove are not large. The minimum value of the transmittance is larger for a ridge than for a groove; as $\phi_0$ increases, so does the transmittance, which is still larger for a ridge than for a groove. The maximum value of the emittance is smaller for a ridge than for a groove; as $\phi_0$ increases, the emittance increases slightly for a ridge, but decreases more significantly for a groove. The maximum value of the reflectance is larger for the ridge than for the groove; as $\phi_0$ increases, the reflectance increases significantly for a ridge, but remains almost the same for a groove. Finally, unitarity (energy conservation) is satisfied with an error smaller than approximately 0.5 % in all cases considered. It is better satisfied for ridges than for grooves, but less well satisfied as $\phi_0$ increases for both cases.

When the amplitude of the surface defect is increased to $|A| = 24$ nm (Fig. 3), the results for $T(\omega)$, $R(\omega)$, $S(\omega)$, and their sum are qualitatively similar to those presented in Fig. 2. However, there are some quantitative differences. The minima in the transmittance of both a ridge and a groove occur at smaller values of this function, but the minimum value of the transmittance is again larger for a ridge than for a groove. The maxima in the emittance and reflectance of both a ridge and a groove occur at larger values of these functions. However, the maximum value of the emittance is larger for a groove than for a ridge, while the maximum value of the reflectance is larger for the ridge than for the groove.

These characteristics of the frequency dependencies of the transmittance, emittance, and reflectance are maintained when the amplitude of the surface defect is increased to $|A| = 36$ nm (Fig. 4).

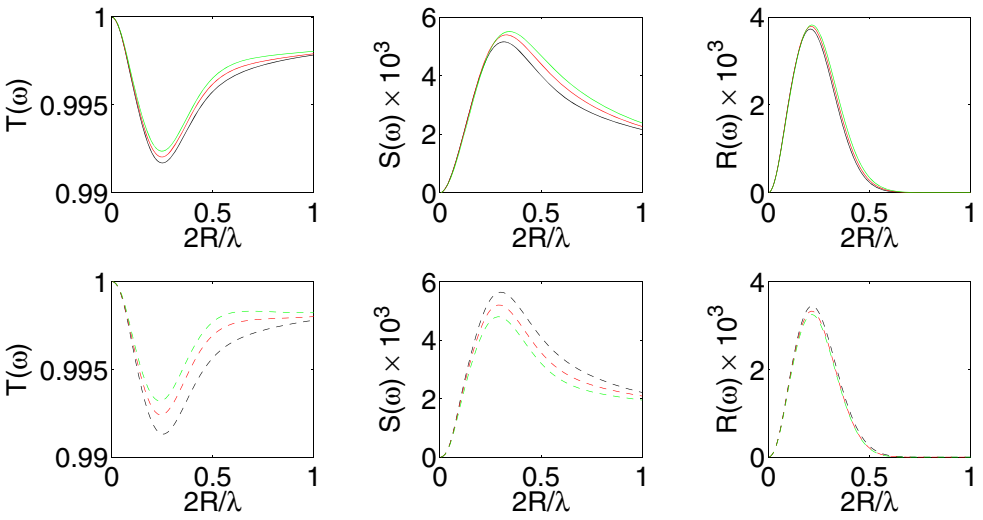


**Fig. 5** The dependence of the transmittance, reflectance, and emittance of a Gaussian ridge or groove on an otherwise planar silver surface on $2R/\lambda$, when a surface plasmon polariton whose wavelength is $\lambda = 600$ nm is incident at an angle $\phi_0 = 0°$ (*black curves*), 5 ° (*red curves*), and 10 ° (*green curves*). The amplitude of the defect is $|A| = 12$ nm. The *solid* and *dashed* curves in each case depict the results for a ridge and a groove, respectively

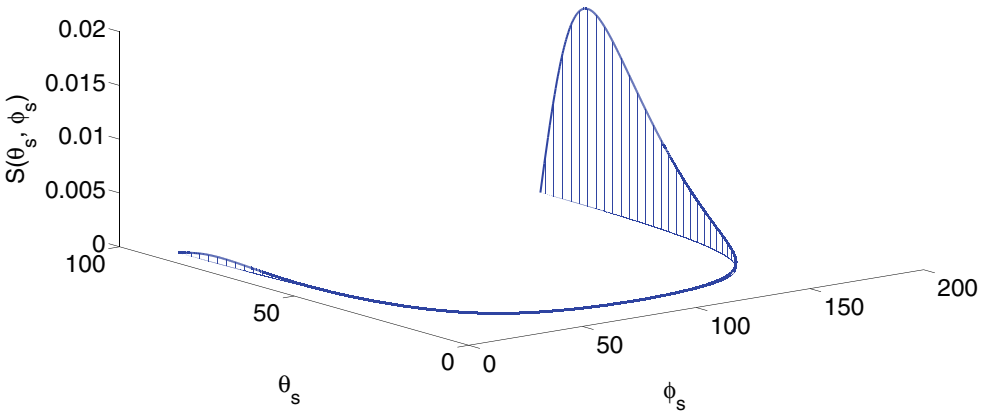


**Fig. 6** Conical scattering of the emittance when a surface plasmon polariton whose wavelength is $\lambda = 600$ nm is incident at an angle $\phi_0 = 10\,^\circ$; on a Gaussian surface defect, defined by Eq. 5.2, on an otherwise planar silver surface. The values of the parameters assumed in obtaining these results are $\omega_p = 11.76 \times 10^{15}\ \mathrm{s}^{-1}$, $R = 30$ nm, and $A = 12$ nm

The frequency at which the maxima and minima of the transmittance, emittance, and reflectance occur is almost unaffected by changes in $|A|$ as $R$ remains fixed, and has a value close to $\omega/\omega_p = 0.45$ in all of the cases considered.

Until now, we have considered spectral dependencies of the transmittance, emittance, and reflectance when the width of the surface defect is fixed and its amplitude is varied. We now consider the transmittance, emittance, and reflectance of the surface defect as functions of its width when its amplitude is fixed, as is the wavelength of the incident surface plasmon polariton. In Fig. 5, we present plots of these functions versus $2R/\lambda$, in the interval $0 \leq 2R/\lambda \leq 1$, when the frequency of the surface plasmon polariton is $\omega/\omega_p = 0.267$ ($\lambda = 600$ nm), while the amplitude of the surface defect is $|A| = 12$ nm. The solid curve (——) and the dashed curve (- - - - -) for each function depict the results obtained for a ridge and a groove, respectively. The angles of incidence considered are 0 (normal incidence [13]), 5, and 10 °. As the angle of incidence increases, so does the transmittance, the emittance decreases (increases), and the reflectivity decreases (increases) for grooves (ridges).

We come now to the angular dependence of the intensity of the field scattered into the vacuum region. Results for scattering from a ridge and from a groove are presented in Figs. 6 and 7, respectively. These results were obtained in the following way. For a chosen value of $\phi_0$, a set of equally spaced values of $\phi_s$ was created within the interval $\sin^{-1}(n(\omega)\sin\phi_0) < \phi_s < \pi - \sin^{-1}(n(\omega)\sin\phi_0)$. For each of these values of $\phi_s$, the corresponding value of $\theta_s$ was determined from the relation $\theta_s = \sin^{-1}(n(\omega)\sin\phi_0/\sin\phi_s)$. Then, for each pair of values $(\theta_s, \phi_s)$ obtained this way, we calculate $S(\theta_s, \phi_s|\omega)$, given by Eq. 3.49, and construct a three-dimensional plot of this function. In plotting $S(\theta_s, \phi_s|\omega)$, in this way, we see that it is confined to a U-shaped curve in the $(\theta_s, \phi_s)$ plane defined by the curve $\theta_s = \sin^{-1}(n(\omega)\sin\phi_0/\sin\phi_s)$. This is a manifestation of the conical nature of the volume electromagnetic field scattered into the vacuum when a surface plasmon polariton is incident obliquely on a line defect. From the results presented in Figs. 6 and 7, we see that for the values of the parameters defining the defects and of the experimental parameters assumed in obtaining these figures, the scattering patterns for scattering from a ridge and from a groove are qualitatively and quantitatively very similar. It is also seen that the scattering from each type of defect is predominantly in the backward direction, i.e., into the region $x_1 < 0$.

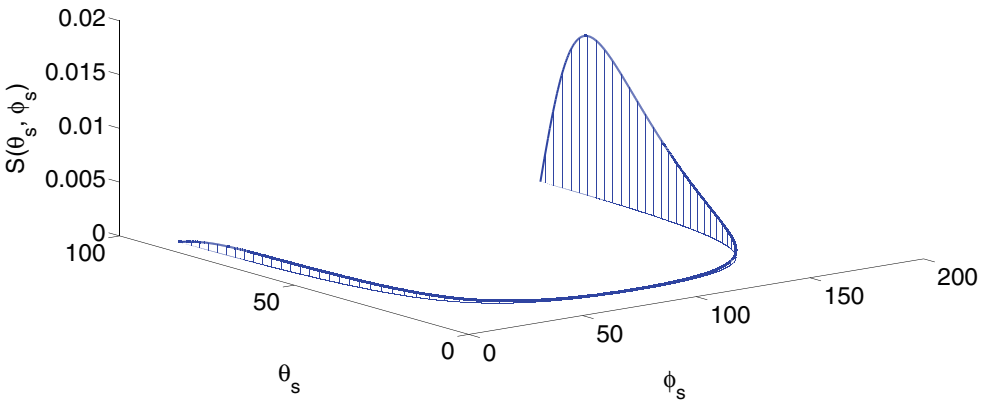


**Fig. 7** The same as Fig. 6, but for $A = -12$ nm

## Discussion and Conclusions

In this paper, we have first derived the reduced Rayleigh equation for the scattering of a surface plasmon polariton incident obliquely on a one-dimensional topographical defect on an otherwise planar metal surface in contact with vacuum. We have then applied this equation to the determination of the scattering coefficients for defects defined by a Gaussian profile function. Two assumptions underlie the present work, namely that the use of the Rayleigh hypothesis is valid, and that the dielectric function of the metal can be assumed to be real. These assumptions have been discussed and justified in prior work [13].

We have studied quantitatively how the frequency dependence of the transmittance, emittance, and reflectance of a ridge differ from those of a groove for a Gaussian surface defect, and have found that these differences are small near normal incidence, but grow larger as the angle of incidence increases. This behavior is more pronounced as the depth of the groove increases. The frequencies at which the spectral dependencies of the transmittance, emittance, and reflectance have their minima or maxima are only very weakly dependent on the values of the parameters $A$ and $R$ that define this surface defect.

With regard to the angular dependence of the scattering patterns of the fields scattered into the vacuum from either a ridge or a groove, the most interesting result is that these patterns are confined to the surface of a cone whose axis lies along the ridge or groove. Thus, the incidence surface plasmon polariton undergoes conical out-of-plane scattering when it impinges obliquely on such a linear topographical surface defect. This result should be verifiable experimentally.

## References


1. Sánchez-Gil JA (1998) Surface defect scattering of surface plasmon polaritons: mirrors and light emitters. Appl Phys Lett 73:3509–3511
2. Sánchez-Gil JA, Maradudin AA (1999) Near-field and far-field scattering of surface plasmon polaritons by one-dimensional surface defects. Phys Rev B 60:8359–8367
3. Sánchez-Gil JA, Maradudin AA (2003) Resonant scattering of surface plasmon polariton pulses by nanoscale metal defects. Opt Lett 28:2255–2257
4. Sánchez-Gil JA, Maradudin AA (2004) Dynamic near-field calculations of surface-plasmon polariton pulses resonantly scattered at sub-micron metal defects. Opt Express 12:883–894
5. Sánchez-Gil JA, Maradudin AA (2005) Surface plasmon polariton scattering from a finite array of nano grooves/ridges: efficient mirrors. Appl Phys Lett 86(1–3):251106
6. Maradudin AA (1994) An impedance boundary condition for a rough surface, pp. 33–45. Topics in Condensed Matter Physics, ed. M. P. Das. Nova Science Publishers, New York
7. Nikitin AY, López-Tejeira F, Martín-Moreno L (2007) Scattering of surface plasmon polaritons by one-dimensional inhomogeneities. Phys Rev B75(1–8):035–129
8. Leskova TA, Maradudin AAE, García-Guerrero E, Méndez ER (2010) The scattering of surface plasmon polaritons by nanoscale surface defects. Fiz Nizkh Temperatur 36:1022–1029
9. Chremmos I (2010) Magnetic field integral equation analysis of surface plasmon scattering by rectangular dielectric channel discontinuities. J Opt Soc Am A27:85–94
10. Brucoli G, Martín-Moreno L (2011) Comparative study of surface plasmon scattering by shallow ridges and grooves. Phys Rev B83(1–11):045–422
11. Brucoli G, Martín-Moreno L (2011) Effect of defect depth on surface plasmon scattering by subwavelength surface defects. Phys Rev B 83(1–10):075–433
12. Kuttge MF, García de Abajo J, Polman A (2009) How grooves reflect and confine surface plasmon polaritons. Opt Express 17:10385–10392
13. Polanco J, Fitzgerald RM, Maradudin AA (2013) Scattering of surface plasmon polaritons by one-dimensional surface defects. Phys Rev B 87:155417–155430
14. Nikitin AY, Martín-Moreno L (2007) Scattering coefficients of surface plasmon polaritons impinging at oblique incidence onto one-dimensional surface relief defects. Phys Rev B 75(1–4): 081–405
15. Petit R, Cadilhac M (1996) Sur la diffraction d'une onde plane par un réseau infiniment conducteur. C R Acad Sci B 262: 468–471
16. Millar RF (1969) On the Rayleigh assumption in scattering by a periodic surface. Proc Camb Philos Soc 65:773–791
17. Hill NR, Celli V (1978) Limits of convergence of the Rayleigh method for surface scattering. Phys Rev B 17: 2478–2481
18. Van den Berg PM, Fokkema JT (1979) The Rayleigh hypothesis in the theory of reflection by a grating. J Opt Soc Am 69: 27–31
19. Van den Berg PM, Fokkema JT (1980) The Rayleigh hypothesis in the theory of diffraction by a perturbation in a plane surface. Radio Sci 15:723–732
20. Schlup WA (1984) On the convergence of the Rayleigh ansatz for hard-wall scattering on arbitrary periodic surface profiles. J Phys A: Math Gen 17:2607–2619
21. DeSanto JA (1981) Scattering from a perfectly reflecting arbitrary periodic surface: an exact theory. Radio Sci 16: 1315–1326
22. Paulick TC (1990) Applicability of the Rayleigh hypothesis to real materials. Phys Rev B 42:2801–2824
23. Millar RF (1973) The Rayleigh hypothesis and a related least-squares solution to scattering problems for periodic surfaces and other scatterers. Radio Sci 8:785–796
24. Rayleigh L (1896) The theory of sound, vol II, 2nd. MacMillan, London, pp 89, 297–311
25. Brown GC, Celli V, Haller M, Marvin A (1984) Vector theory of light scattering from a rough surface: Unitary and reciprocal expansions. Surf Sci 136:381–397
26. Maradudin AA, Mills DL (1976) The attenuation of Rayleigh surface waves by surface roughness. Ann Phys (N. Y.) 100:262–309. Appendix D
27. Press WH, Teukolsky SA, Vetterling WT, Flannery BP (1992) Numerical recipes. Cambridge University Press, Cambridge, UK, pp 109–110
28. Press WH, Teukolsky SA, Vetterling WT, Flannery BP (1992) Numerical recipes, Cambridge University Press, Cambridge, UK. Chapter 2